OPEN ACCESS

Feshbach resonances in ultracold ^{39}K

New Journal of Physics
The open–access journal for physics

Feshbach resonances in ultracold ^{39}K

Chiara D'Errico[1], Matteo Zaccanti[1,2], Marco Fattori[3,1], Giacomo Roati[1,2,4], Massimo Inguscio[1,2,4], Giovanni Modugno[1,2,4] and Andrea Simoni[5]

[1] LENS and Dipartimento di Fisica, Università di Firenze, Via Nello Carrara 1, 50019 Sesto Fiorentino, Italy
[2] INFN, Via Sansone 1, 50019 Sesto Fiorentino, Italy
[3] Museo Storico della Fisica e Centro Studi e Ricerche 'Enrico Fermi', Compendio del Viminale, 00184 Roma, Italy
[4] CNR-INFM, Via Sansone 1, 50019 Sesto Fiorentino, Italy
[5] Laboratoire de Physique des Atomes, Lasers, Molécules et Surfaces, UMR 6627 du CNRS and Université de Rennes, 35042 Rennes Cedex, France
E-mail: andrea.simoni@univ-rennes1.fr

New Journal of Physics **9** (2007) 223
Received 21 May 2007
Published 11 July 2007
Online at http://www.njp.org/
doi:10.1088/1367-2630/9/7/223

Abstract. We discover several magnetic Feshbach resonances in collisions of ultracold ^{39}K atoms, by studying atom losses and molecule formation. Accurate determination of the magnetic-field resonance locations allows us to optimize a quantum collision model for potassium isotopes. We employ the model to predict the magnetic-field dependence of scattering lengths and of near-threshold molecular levels. Our findings will be useful to plan future experiments on ultracold ^{39}K atoms and molecules.

Contents

1. Introduction 2
2. Experiment 2
3. Theoretical analysis 5
4. Outlook 10
Acknowledgments 12
References 12

PII: S1367-2630(07)50769-X

1. Introduction

Control of the isotropic interaction in ultracold atomic gases [1,2] is revealing itself as a fundamental tool to explore a variety of fundamental phenomena. Tuning the interaction between two different hyperfine states in Fermi gases via magnetic Feshbach resonances has permitted unprecedented investigations of the BEC–BCS crossover [3]. Mean-field effects such as collapse [4] or formation of bright solitons [5] have been demonstrated in Bose–Einstein condensates with tunable interactions. Homonuclear Feshbach resonances have also been successfully used to convert atomic gases in molecular Bose–Einstein condensates [6], to produce strongly correlated quantum phases [7, 8] and to observe Efimov trimer states [9]. Analogous experiments with heteronuclear systems are in progress [10].

Feshbach resonances have been discovered in most alkali species, including Li [11], Na [2], K [12] Rb [13], Cs[14], in chromium [15] and in a few alkali mixtures [16]. In the case of potassium, intensive study of two specific resonances in fermionic ^{40}K [12] has been motivated by possible applications to fermionic superfluidity. Although ultracold samples of the bosonic isotopes ^{41}K and ^{39}K have also been produced [17, 18], magnetic Feshbach resonances have not yet been investigated in these systems. Moreover, only limited theoretical predictions exist for these isotopes [19, 20].

We report here the first experimental study of Feshbach resonances in an ultracold ^{39}K gas. We discover several resonances in three different hyperfine states and measure their magnetic-field location by observing on-resonance enhancement of inelastic three-body losses and molecule formation. Each hyperfine state of interest presents at least one broad Feshbach resonance which can be used to tune with high accuracy the interaction in a ^{39}K Bose–Einstein condensate [21].

The observed resonance locations are used to construct an accurate theoretical quantum model which explains both present and pre-existing observations [12]. The model allows us to compute relevant quantities such as background scattering lengths and resonance widths. In addition, we fully characterize hyperfine-coupled molecular levels near the dissociation limit. Knowledge of molecular parameters is essential for understanding experiments performed in the strongly interacting regime. It is also important for implementing schemes of molecule formation and for the interpretation of their properties.

2. Experiment

The apparatus and techniques we use to prepare ultracold samples of ^{39}K atoms have already been presented in detail elsewhere [21] and are only briefly summarized here. We begin by preparing a mixture of ^{39}K and ^{87}Rb atoms in a magneto-optical trap at temperatures of the order of a few 100 μK. We simultaneously load the two species in a magnetic potential in their stretched Zeeman states $|F = 2, m_F = 2\rangle$ and perform 25 s of selective evaporation of rubidium on the hyperfine transition at 6.834 GHz. Potassium is sympathetically cooled through interspecies collisions [18]. When the mixture temperature is below 1 μK it is transferred to an optical potential. This is created with two focused laser beams at a wavelength $\lambda = 1030$ nm, with beam waists of about 100 μm and crossing in the horizontal plane.

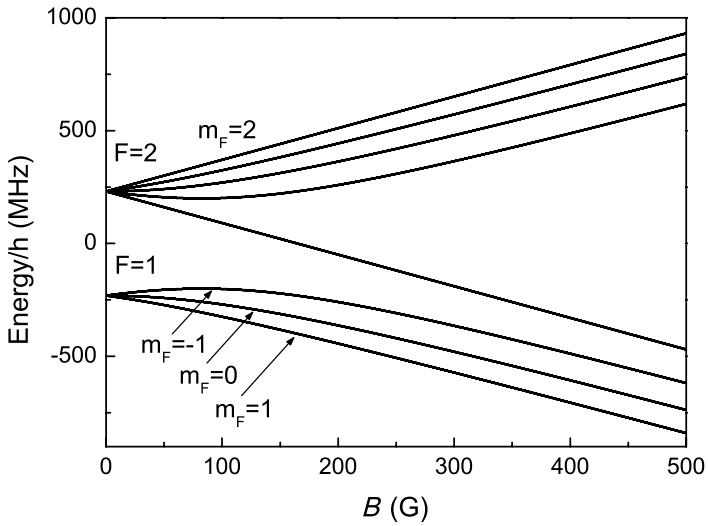

Figure 1. Energy levels of ^{39}K atoms in a magnetic field. Levels are labelled using zero-field quantum numbers.

In this work, we have studied Feshbach resonances in all the states immune from spin-exchange collisions, the three Zeeman sublevels of the $F = 1$ manifold[6]. The level structure of ^{39}K in a magnetic field is shown in figure 1. The atoms are initially prepared in the $|1, 1\rangle$ state by adiabatic rapid passage over the hyperfine transition around 462 MHz [22] in a 10 G homogeneous magnetic field. To further cool the sample, we transfer also Rb to its ground state, and we lower the optical trap depth by exponentially decreasing the laser power in 2.4 s. During the forced evaporation of both species we increase the K–Rb elastic cross-section by applying a homogeneous magnetic field of 316 G, close to an interspecies Feshbach resonance [21]. With this technique we are able to cool the K sample to a final temperature in the range 150–500 nK. At these temperatures the sample is not yet quantum degenerate. Once the K sample has been prepared to the desired temperature, Rb is selectively removed from the trap using a resonant light pulse. To transfer the atoms in the two excited states of the $F = 1$ manifold, we use a radio-frequency sweep. For the transfer from $|1, 1\rangle$ to $|1, -1\rangle$ we apply a 10 G field and use a radio-frequency sweep around 7.6 MHz. For the transfer from $|1, 1\rangle$ to $|1, 0\rangle$ we use instead a 38.5 G field and a radio-frequency sweep around 28.5 MHz. After the atoms have been prepared in a given state (this typically requires from 10 to 30 ms, depending on the final state) we change the homogeneous field in a few ms and actively stabilize it to any desired value in the 0–1000 G range with an accuracy of about 100 mG. We calibrate the field by means of microwave and RF spectroscopy on two different hyperfine transitions of Rb.

Feshbach resonances are detected as an enhancement of losses. In the proximity of a Feshbach resonance, the scattering length can be parametrized as [1]

$$a(B) = a_{\mathrm{bg}}\left(1 - \frac{\Delta}{B - B_0}\right), \tag{1}$$

[6] Indication of Feshbach resonances in an unpolarized sample of ^{39}K atoms has been obtained also in an experiment at the University of Innsbruck: communication at Wilhelm und Else Heraeus-Seminar on Cold Molecules, Bad Honnef (Germany), 2006.

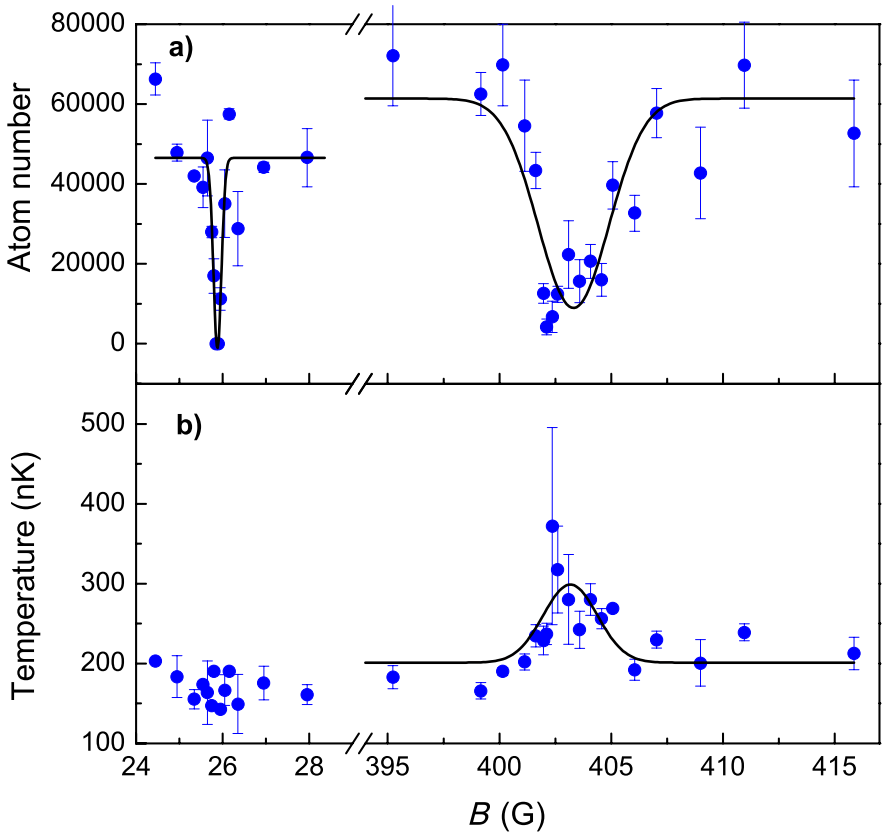

Figure 2. Experimental determination of Feshbach resonances in the $|1, 1\rangle$ state of ^{39}K: (a) remaining atom number; (b) sample temperature. The hold time for the low field (high field) resonance was 480 ms (36 ms). The curves are phenomenological fits with Gaussian distributions.

where a_{bg} is the background scattering length, Δ is the resonance width, and B_0 the resonance centre. The resonance width Δ represents the separation between B_0 and the location where the scattering length crosses zero. As $a(B)$ diverges, two- and three-body inelastic rates are enhanced, resulting in atom loss from the trap and heating [23]. This potassium isotope presents both very narrow ($\Delta < 0.5$ G) and very broad resonances ($\Delta \sim 50$ G). Examples of two such resonances in the $|1, 1\rangle$ state are shown in figure 2. In the present experiment the magnetic field was brought to a variable value in the range 0–500 G, and held there for a given time. Both field and trapping laser were then switched off and atom number and temperature were measured through standard absorption imaging. The narrow resonance around 26 G gives rise to a rather sharp, symmetric loss features centred at B_0. Conversely, the broad resonance around 400 G corresponds with broader, highly asymmetric loss and heating features. Possible sources of asymmetry will be discussed later. The different strength of the two resonances is indicated by the different hold time required to have about 90% peak losses; this amounts to 480 ms for the narrow resonance[7] and 36 ms for the broad one.

[7] The long hold time used for the narrow resonance explains the absence of heating: after a collisional event and the subsequent heating, the system has time to evaporate and rethermalize to a lower temperature.

Table 1. Experimental magnetic-field positions $B_{\rm exp}$ and theoretically calculated positions $B_{\rm th}$, widths Δ, magnetic moments s, background scattering length $a_{\rm bg}$, and approximate quantum numbers (see text) of ^{39}K $\ell = 0$ Feshbach resonances for different m_{Fa}, m_{Fb} Zeeman sublevels.

m_{Fa}, m_{Fb}	$B_{\rm exp}$ (G)	$B_{\rm th}$(G)	$-\Delta_{\rm th}$ (G)	$-s$ ($\mu_{\rm B}$)	$a_{\rm bg}(a_0)$	(SIf) or $\{SIM_S\}$
1, 1	25.85(10)	25.9	0.47	1.5	−33	(133)
	403.4(7)	402.4	52	1.5	−29	
		745.1	0.4	3.9	−35	{113}
	752.3(1)	752.4	0.4	3.9	−35	{111}
0, 0	59.3(6)	58.8	9.6	0.83	−18	(133)
	66.0(9)	65.6	7.9	0.78	−18	(111)
		471	72	1.22	−28	
		490	5	1.70	−28	
		825	0.032	3.92	−36	{113}
		832	0.52	3.90	−36	{111}
−1, −1	32.6(1.5)	33.6	−55	−1.9	−19	(112)
	162.8(9)	162.3	37	1.2	−19	(133)
	562.2(1.5)	560.7	56	1.4	−29	

The same procedure was repeated for the two other hyperfine states. In total we have studied eight Feshbach resonances, whose centres are listed in table 1. For most broad resonances, we have found an asymmetry in loss and heating profiles similar to the one shown in figure 2. In the absence of a precise model of our system, we have fitted the experimental profiles with a single Gaussian to determine the resonance centres $B_{\rm exp}$. The error we give on $B_{\rm exp}$ is the quadratic sum of our magnetic-field accuracy and of the error deriving from the fit, which is usually dominating for broad loss profiles.

3. Theoretical analysis

Early information about K collision properties was obtained from the analysis of photoassociation (PA) spectra of the bosonic isotope ^{39}K, see [24, 25]. The collision model has then been refined by theoretically analysing observed shape [26] and Feshbach resonances [12] in fermionic ^{40}K. Subsequently, the Nist/Connecticut groups have inferred potential parameters from two-photon spectroscopy of ^{39}K near-dissociation molecular levels [27]. Finally, cold collision (CC) measurements have been performed on ^{39}K [18]. These different determinations are summarized in table 2 (scattering quantities are defined in the following).

Our present collision model comprises adiabatic Born–Oppenheimer singlet $X^1\Sigma_{\rm g}^+$ and triplet $a^3\Sigma_{\rm u}^+$ interaction potentials determined from spectroscopic data [29, 30]. The adiabatic potentials asymptotically correlate with the well known dispersion plus exchange analytical form

$$V(^{1,3}\Sigma_{\rm g,u}^+) \to -\frac{C_6}{R^6} - \frac{C_8}{R^8} - \frac{C_{10}}{R^{10}} \mp A R^{\alpha} {\rm e}^{-\beta R}, \tag{2}$$

where $\alpha = 7/\beta - 1$, $\beta = \sqrt{8I}$, I is the atomic first ionization energy in hartrees [31] and A is a positive constant. Hyperfine interactions are mostly important at large internuclear separation

Table 2. Comparison of collisional parameters for ^{39}K determined from CC and PA spectroscopy of ultracold atoms. Some analyses did not determine the value of C_6, which was taken from theory (value and reference are then reported in the third column of the table). The δC_6 is the shift in C_6 from the value $C_6 = 3897$ a.u. of [28].

Reference	$a_S(a_0)$	$a_T(a_0)$	C_6(a.u.)
This work	138.90 ± 0.15	-33.3 ± 0.3	3921 ± 8
CC [18]		-51 ± 7	
CC [12]	139.4 ± 0.7	-37 ± 6	3927 ± 50
PA [27]		-33 ± 5	3897 ± 15 [28]
CC [26]		$>-80, <-28$	3813 [33]
PA [25]	$>90, <230$	$>-60, <15$	3813 [33]
PA [24, 19]	140^{+6}_{-9}	$-21 - 0.045\ \delta C_6 \pm 20$	

and are safely approximated by their atomic limit. A short-range correction is finally added to the adiabatic potentials to model the data [19].

The experimental resonance locations are used in a *weighted* least square procedure to determine the correction size. The resulting optimized potentials are parametrized in terms of s-wave singlet a_S and triplet a_T scattering lengths and of the long-range parameters $C_n, n = 6, 8, 10$. Resonance positions are mainly sensitive to the leading van der Waals coefficient C_6, which along with the $a_{S,T}$ is a fitting parameter in our procedure. In order to obtain maximum constraint we also include in the empirical data the positions of two already known ^{40}K resonances [12], and a p-wave resonance we have recently discovered at 436.3(5) G in collisions of ^{40}K $|9/2, 7/2\rangle$ atoms. We use the same potential for the two isotopes assuming thereby the validity of the Born–Oppenheimer approximation. The result of the fit is: $a_S = (138.90 \pm 0.15)a_0$, $a_T = (-33.3 \pm 0.3)a_0$, and $C_6 = (3921 \pm 8)$ a.u. The final reduced χ^2 has a value of only 0.52. Our singlet–triplet scattering lengths agree well with previous determinations (see table 1) and represent an improvement of more than one order of magnitude in a_T. The C_6 agrees to one standard deviation with the accurate value of Derevianko *et al* [28], $C_6 = 3897 \pm 15$ a.u. The singlet-triplet scattering lengths of ^{40}K computed with the present model are 104.56 ± 0.10 and 169.7 ± 0.4, in very good agreement with [12].

A magnetic Feshbach resonance arises at a value B_0 of the magnetic field when the energy of the separated atom pair becomes degenerate with the energy of a molecular bound level. Scattering near a magnetic resonance is fully characterized [32] by assigning B_0, Δ, the background scattering length a_{bg}, the C_6 coefficient, the magnetic moment s of the molecule associated to the resonance with respect to free atoms

$$s = \frac{\partial(E_{at} - E_{mol})}{\partial B}, \tag{3}$$

where E_{at} and E_{mol} represent the energy of the separated atoms and of the molecule, respectively, and the derivative is taken away from resonance. Parameters values for observed and theoretically predicted resonances are found in table 1.

In cases where resonances are overlapping (i.e. when the magnetic width is comparable to their magnetic field separation) we will parametrize the effective scattering length with one

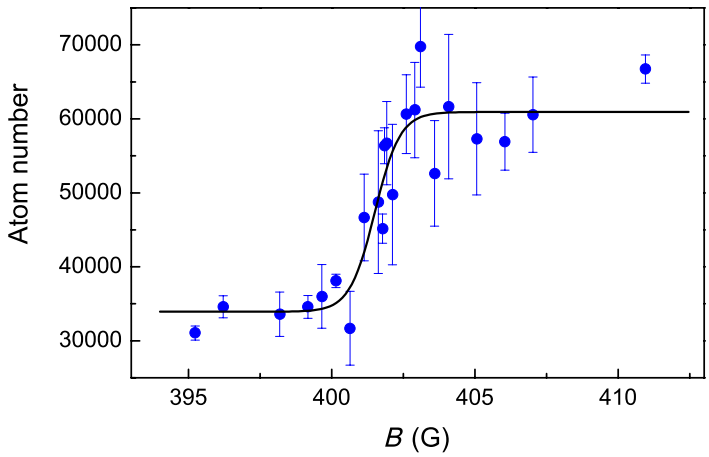

Figure 3. Molecule formation at the broadest Feshbach resonances in the $|1, 1\rangle$ state of ^{39}K. The magnetic field is linearly swept from 410 G to a final field B in 2 ms. The resonance centre $B_0 = 401.5(5)$ G is determined by fitting the atom number with a Boltzmann growth function.

background parameter $a_{\rm bg}$, two widths Δ_i and two positions $B_{0,i}$ $(i = 1, 2)$ as

$$a(B) = a_{\rm bg}\left(1 - \frac{\Delta_1}{B - B_{0,1}} - \frac{\Delta_2}{B - B_{0,2}}\right). \tag{4}$$

This expression clearly reduces to equation (1) when the resonances are isolated, $|B_{0,2} - B_{0,1}| \gg \Delta_1, \Delta_2$.

Comparison of experimental and theoretical resonance locations in table 1 indicates that all measured resonances with large Δ feature an asymmetric profile. In all these cases, the centre of the gaussian fit to the loss profiles is indeed shifted towards the region of negative scattering lengths, as in the case reported in figure 2. This can be understood by noting that in the proximity of a Feshbach resonance the three-body loss coefficient is larger for negative scattering lengths than for positive ones [34]. Other possible contributions to such asymmetry are mean field effects for large positive and negative scattering lengths close to the resonance centre. For $B > B_0$ the density should indeed increase with respect to the noninteracting value, while for $B < B_0$ it should decrease. This would accordingly vary the loss rates through their density dependencies and promote losses on region with $B > B_0$. In the absence of a detailed model of our finite temperature system, we performed an independent experiment to determine the centre of the broad ground-state resonance in figure 2, by studying molecule association. We used the standard technique of adiabatic magnetic-field sweeps over the resonance from the atomic to the molecular side [6]. The system was initially prepared at a magnetic field well above the resonance centre, $B_i = 410$ G, at a temperature of 220 nk. The field was then swept to a final lower field B in 2 ms, left to stabilize for 0.1 ms, then suddenly switched off. As shown in figure 3, as B crosses the resonance the atom number drops to about 50% of the initial value, in the absence of any heating of the system. This indicates that a fraction of the atoms are converted into weakly-bound molecules. The molecules are very rapidly lost from the trap via inelastic collisions. A fit using a Boltzmann growth function gives a resonance centre of $B_0 = 401.5(5)$ G. This is almost 2 G lower than the centre of the broad loss profile, and is consistent with both

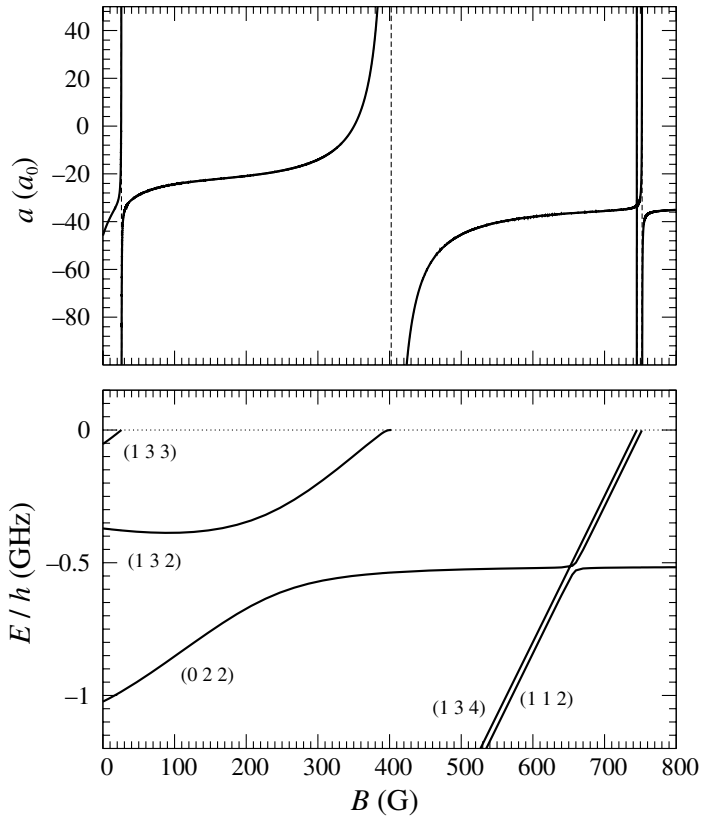

Figure 4. Upper panel: magnetic field dependence of the effective scattering length for $|1, 1\rangle + |1, 1\rangle$ ^{39}K collisions. Dashed lines indicate the resonance positions. Lower panel: near-threshold molecular levels for $m_f = 2$. Zero energy is taken at the separated atoms limit. The quantum numbers shown in brackets (SIf) are good in general only for weak magnetic fields, see text.

$B_{\rm th} = 402.4(2)$ G and the value at which the maximum atom loss and heating is seemingly taking place in the data shown in figure 2, $B = 402.2(2)$ G. This agreement confirms that the global fit we make is able to accurately fix the position of all resonances, although the broad resonances centres are individually determined with poorer accuracy by loss measurements.

In order to complete the resonance characterization, we now discuss approximate quantum labels of the Feshbach molecule. Neglecting weak dipolar interactions and for vanishing magnetic field the internal angular momentum $\vec{f} = \vec{S} + \vec{I}$ is conserved. Here $\vec{S}$ and $\vec{I}$ are the electronic and nuclear spin, respectively. Moreover, because of the small hyperfine splitting of ^{39}K with respect to the splitting between neighbouring singlet-triplet levels, S and I are approximately good quantum numbers at least for low B. Because of the spherical symmetry of the problem, the orbital angular momentum $\vec{\ell}$ of the atoms is also a conserved quantity. All of our observed resonances have $\ell = 0$. Zero-energy quantum numbers are shown in figures (4–6) for the closest to dissociation levels.

As the field increases these quantum numbers are no longer any good. In fact, for intense magnetic fields the Zeeman energy becomes larger than both the hyperfine and the singlet/triplet vibrational splitting. In this regime $\vec{S}$ and $\vec{I}$ uncouple and precede independently about the

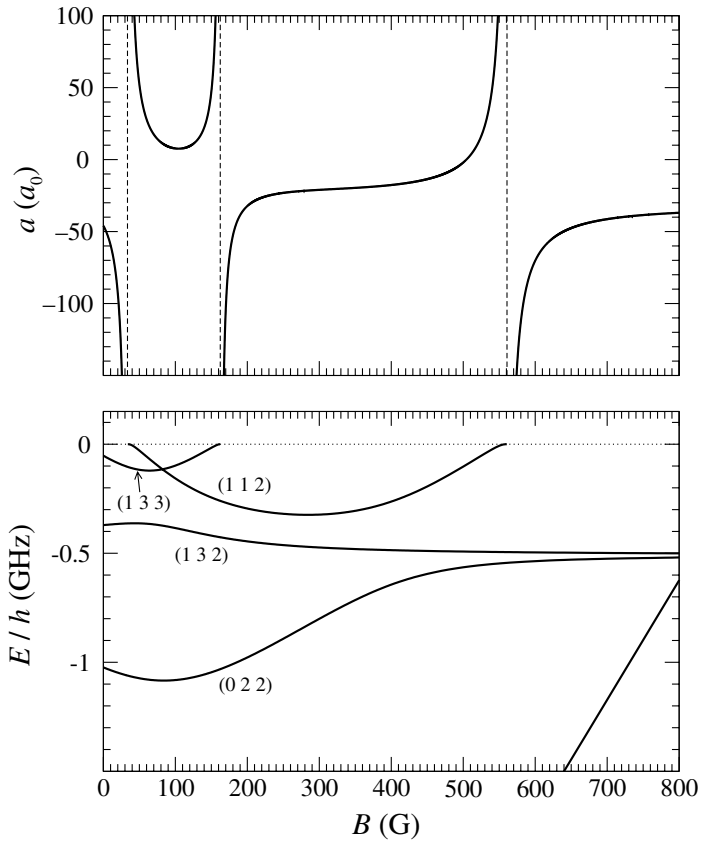

Figure 5. Same as figure 4 but for $|1, 0\rangle$ atoms and $m_f = 0$.

magnetic field. The molecular quantum state can then be identified by S, I and by the spin projections M_S and M_I on the quantization axis.

In the intermediate regime neither coupling scheme is accurate as singlet and triplet levels are sufficiently close to be strongly mixed by off-diagonal hyperfine interactions. However, axial symmetry of the problem enforces conservation of the magnetic quantum number m_f (i.e. the axial projection of $\vec{f}$). Examples of resonances arising from such mixed levels are the 402 G (figure 4), the 471 and 490 G (figure 5), and the 561 G (figure 6) features. One can note from the figures broad avoided crossings caused by spin-exchange interaction between levels of different S and the same f. An approximate assignment constructed for low and high field by averaging the appropriate spin operators on the molecular wavefunctions is presented in table 1. Resonances arising from mixed levels are left unassigned. Their zero-field correlation can be easily inferred from the figures.

One should also note that the quantum numbers discussed above are in principle only valid away from resonance. Actually, there is always a range of magnetic fields near resonance where the amplitude of the molecular state is almost entirely transferred to the open background channel [32], which is not represented by the same quantum numbers as the molecule. This magnetic field region can be estimated as [32, 35]

$$\frac{B - B_0}{\Delta} \ll \frac{m a_{\mathrm{bg}}^2 s \Delta}{\hbar^2}, \tag{5}$$

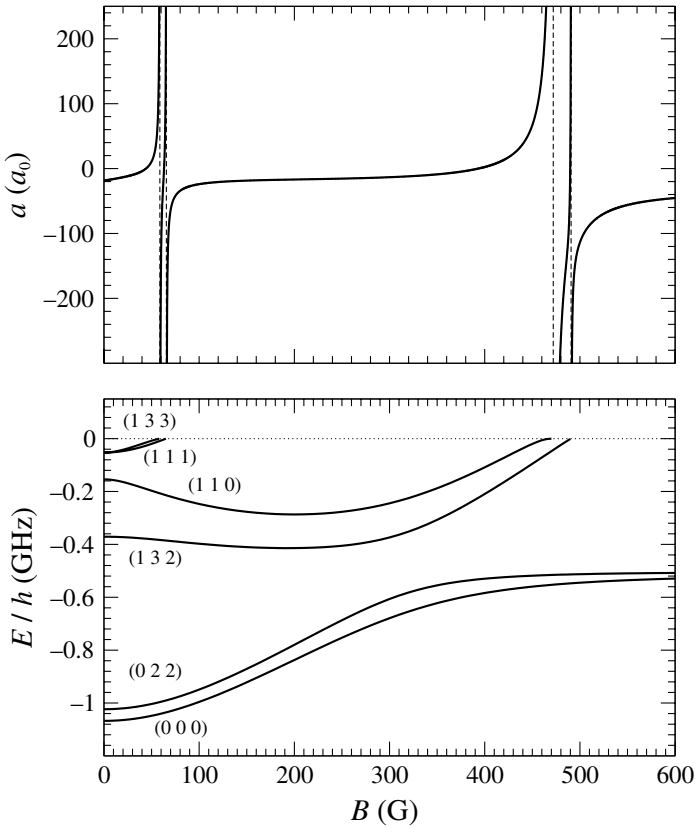

Figure 6. Same as figure 4 but for $|1, -1\rangle$ atoms and $m_f = -2$.

with m the atomic mass. Resonances for which the right hand side of equation (5) is $\gg 1$ are termed open channel dominated. The present resonances range from closed channel dominated (rhs $\ll 1$) to an intermediate situation (rhs $\simeq 1$). When condition (5) is fulfilled, the energy of the molecule takes the form

$$E_{\mathrm{mol}}(B) - E_{\mathrm{at}}(B) = -\frac{\hbar^2}{m\,[a(B) - l_{\mathrm{vdW}}]^2}, \qquad l_{\mathrm{vdW}} = \frac{1}{2}\left(\frac{mC_6}{\hbar^2}\right)^{1/4}, \tag{6}$$

see e.g. [32, 35], and scattering can be described in terms of a single effective channel. The l_{vdW} is the typical length associated to a R^{-6} interaction. The validity of estimate (5) is confirmed by inspection of figures (4)–(6) in which the asymptotic behaviour (6) is only attained in a region of a few G even near the broadest resonances with $\Delta \simeq 50$ G. Outside this region, at least a two-channel model based on the parameters reported in table 1 is needed [32].

4. Outlook

As shown in table 2, at least one broad resonance ($\Delta \sim 50$ G) is available for ^{39}K atoms prepared in each level of the lowest hyperfine manifold. By virtue of their large width such resonances can be used to precisely tune the interactions in an ultracold sample. In fact we have recently demonstrated how to exploit the broad resonance at 402 G in the absolute ground state in order to produce a stable ^{39}K Bose–Einstein condensate with widely tunable properties [21]. This system

Table 3. Theoretically calculated positions $B_{\rm th}$ and widths Δ of $\ell = 0$ Feshbach resonances for ^{41}K. Only resonances with $\Delta > 10^{-3}$ G are reported.

m_{Fa}, m_{Fb}	$B_{\rm th}$(G)	$\Delta_{\rm th}$ (G)
1, 1	408.7	0.03
	660.1	0.2
	856.8	0.002
0, 0	451.5	0.01
	702.7	0.3
	900.1	0.002
−1, −1	51.4	−0.3
	499.9	0.004
	747.0	0.2
	945.6	0.002

might allow one to study a broad range of phenomena ranging from atom interferometry with weakly interacting condensates and strongly-correlated systems in optical lattices to molecular quantum gases and Efimov physics.

The small background scattering length makes this system particularly appropriate for the exploration of regimes of weak interactions. At the zero-crossings associated to broad resonances one can indeed achieve a precise control of a around zero in a Bose–Einstein condensate. For example, at the zero-crossing location (350.4 ± 0.4) for $|1, 1\rangle + |1, 1\rangle$ collisions, the model predicts a small magnetic-field sensitivity $\mathrm{d}a/\mathrm{d}B \simeq 0.55\, a_0$/G. This would imply a control of a to zero within $0.05a_0$ for a field stability of 0.1 G. The other broad resonances for collisions of $|1, 0\rangle$ and of $|1, -1\rangle$ atoms can likewise be used to produce and manipulate a ^{39}K condensate. For example, we have already experimentally verified that a condensate can be produced by evaporative cooling exploiting either low-field resonance in $|1, -1\rangle$. Comparing figure 1 and figure 5 one should note how the magnetic-field region around 80 G in which the scattering length of this state is small and positive ($a \simeq 11a_0$) coincides with the maximum in energy of the state. Here an ultracold ^{39}K sample would therefore present at the same time relatively weak interatomic interactions and nearly vanishing magnetic moment. This peculiar combination is clearly interesting for interferometric applications and is worth further investigation.

Molecule formation in ^{39}K condensates can also be studied, provided a three-dimensional optical lattice is employed to prevent collapse of the condensate on the atomic side of the resonances and to shield inelastic decay of molecules [36]. Also Feshbach resonances due to molecular states with $\ell \neq 0$ are in principle present in this system, and will be the subject of future investigation.

Our accurate analysis on ^{39}K can also be used to calculate the magnetic-field dependent scattering length of the other bosonic isotope, ^{41}K. Bose–Einstein condensation of this species can be achieved without the need of Feshbach resonances, because of the naturally positive scattering length [17]. Our analysis shows that a few resonances exist for magnetic fields in the range 0–1000 G, although they are much narrower than in ^{39}K. This makes ^{41}K less interesting for applications where a precise tuning of the interactions is needed. Positions and widths of Feshbach resonances calculated for our best-fit parameters in the $F = 1$ manifold are reported in table 3.

In conclusion, we have presented a detailed analysis of Feshbach resonances in ultracold ^{39}K atoms. The full characterization of collisional parameters, Feshbach resonances and molecular levels we provide here should be important for planning and interpreting future experiments with ultracold bosonic potassium. The broad Feshbach resonances available in ^{39}K atoms are interesting for precise control of the interaction in a Bose–Einstein condensate over a broad range, and for experiments on ultracold molecules.

Acknowledgments

We thank the whole LENS Quantum Gases group for useful discussions and E Tiesinga for providing the initial potassium potential subroutine. This work was supported by MIUR, by EU under contracts HPRICT1999-00111 and MEIF-CT-2004-009939, by Ente CRF, Firenze and by CNISM, Progetti di Innesco 2005.

References

[1] Tiesinga E, Verhaar B J and Stoof H T C 1993 *Phys. Rev.* A **47** 4114
[2] Inoyue S, Andrews M R, Stenger J, Miesner H-J, Stamper-Kurn D M and Ketterle W 1998 *Nature* **392** 151
[3] Regal C A *et al* 2004 *Phys. Rev. Lett.* **92** 040403
Chin C *et al* 2004 *Science* **305** 1128
Bourdel T *et al* 2004 *Phys. Rev. Lett.* **93** 050401
Partridge G B *et al* 2005 *Phys. Rev. Lett.* **95** 020404
Zwierlein M W*et al* 2005 *Nature* **435** 1047
[4] Roberts J L, Claussen N L, Cornish S L, Donley E A, Cornell E A and Wieman C E 2001 *Phys. Rev. Lett.* **86** 4211
[5] Khaykovich L, Schreck F, Ferrari G, Bourdel T, Cubizolles J, Carr L D, Castin Y and Salomon C 2002 *Science* **296** 1290
Strecker K E, Partridge G B, Truscott A G and Hulet R G 2002 *Nature* **417** 150
[6] Jochim S, Bartenstein M, Altmeyer A, Hendl G, Riedl S, Chin C, Hecker Denschlag J and Grimm R 2003 *Science* **302** 2101
[7] Volz T, Syassen N, Bauer D M, Hansis E, Durr S and Rempe G 2006 *Nat. Phys.* **2** 692
[8] Winkler K, Thalhammer G, Lang F, Grimm R, Hecker Denschlag J, Daley A J, Kantian A, Buechler H P and Zoller P 2006 *Nature* **441** 853
[9] Kraemer T, Mark M, Waldburger P, Danzl J G, Chin C, Engeser B, Lange A D, Pilch K, Jaakkola A, Naegerl H-C and Grimm R 2006 *Nature* **440** 315
[10] Zaccanti M, D'Errico C, Ferlaino F, Roati G, Inguscio M and Modugno G 2006 *Phys. Rev. A* **74** 041605(R)
Ospelkaus S, Ospelkaus C, Humbert L, Sengstock K, Bongs K 2006 *Phys. Rev. Lett.* **97** 120403
Ospelkaus C, Ospelkaus S, Humbert L, Ernst P, Sengstock K and Bongs K 2006 *Phys. Rev. Lett.* **97** 120402
[11] Khaykovich L, Schreck F, Ferrari G, Bourdel T, Cubizolles J, Carr L D, Castin Y and Salomon C 2002 *Science* **296** 1290
Strecker K E, Partridge G B, Truscott A G and Hulet R G 2002 *Nature* **417** 150
Jochim S, Bartenstein M, Hendl G, Hecker Denschlag J, Grimm R, Mosk A and Weidemüller M 2002 *Phys. Rev. Lett.* **89** 273202
[12] Loftus T, Regal C A, Ticknor C, Bohn J L and Jin D S 2002 *Phys. Rev. Lett.* **88** 173201
Regal C A, Ticknor C, Bohn J L and Jin D S 2003 *Phys. Rev. Lett.* **90** 053201

[13] Roberts J L, Claussen N R, Burke J P Jr, Greene C H, Cornell E A and Wieman C E 1998 *Phys. Rev. Lett.* **81** 5109
Marte A, Volz T, Schuster J, Dürr S, Rempe G, van Kempen E G M and Verhaar B J 2002 *Phys. Rev. Lett.* **89** 283202
[14] Chin C, Vuletic V, Kerman A J and Chu S 2002 *Phys. Rev. Lett.* **85** 2717
[15] Werner J, Griesmaier A, Hensler S, Stuhler J, Pfau T, Simoni A and Tiesinga E 2005 *Phys. Rev. Lett.* **94** 183201
[16] Stan C A, Zwierlein M W, Schunck C H, Raupach S M F and Ketterle W 2004 *Phys. Rev. Lett.* **93** 143001
Inouye S, Goldwin J, Olsen M L, Ticknor C, Bohn J L and Jin D S 2004 *Phys. Rev. Lett.* **93** 183201
Ferlaino F, D'Errico C, Roati G, Zaccanti M, Inguscio M, Modugno G and Simoni A 2006 *Phys. Rev.* A **73** 040702(R)
[17] Modugno G, Ferrari G, Roati G, Riboli F, Brecha R J, Simoni A and Inguscio M 2001 *Science* **294** 1320
Modugno G, Modugno M, Riboli F, Roati G and Inguscio M 2002 *Phys. Rev. Lett.* **89** 190404
[18] De Sarlo L, Maioli P, Barontini G, Catani J, Minardi F and Inguscio M 2007 *Phys. Rev.* A **75** 022715
[19] Bohn J, Burke J P Jr, Greene C H, Wang H, Gould P L and Stwalley W C 1999 *Phys. Rev.* A **59** 3660
[20] Tiesinga E private communication
[21] Roati G, Zaccanti M, D'Errico C, Catani J, Simoni A, Modugno M, Inguscio M and Modugno G *Preprint* cond-mat/0703714
[22] Arimondo E, Inguscio M and Violino P 1977 *Rev. Mod. Phys.* **49** 31
[23] Weber T, Herbig J, Mark M, Nägerl H-C and Grimm R 2003 *Phys. Rev. Lett.* **91** 123201
Fedichev P O, Reynolds M W and Shlyapnikov G V 1996 *Phys. Rev. Lett.* **77** 2921
[24] Burke J P Jr, Greene C H, Bohn J L, Wang H, Gould P L and Stwalley W C 1999 *Phys. Rev.* A **60** 4417
[25] Williams C J, Tiesinga E, Julienne P S, Wang H, Stwalley W C and Gould P L 1999 *Phys. Rev.* A **60** 4427
[26] De Marco B, Bohn J L, Burke J P Jr, Holland M and Jin D S 1999 *Phys. Rev. Lett.* **82** 4208
[27] Wang H, Nikolov A N, Ensher J R, Gould P L, Eyler E E, Stwalley W C, Burke J P Jr, Bohn J L, Greene C H, Tiesinga E, Williams C J and Julienne P S 2000 *Phys. Rev.* A **62** 052704
[28] Derevianko A, Johnson W R, Safronova M S and Babb J F 1999 *Phys. Rev. Lett.* **82** 3589
[29] Amiot C, Verges J and Fellows C E 1995 *J. Chem. Phys.* **103** 3350
[30] Zhao G, Zemke W T, Kim J T, Wang H, Bahns J T, Stwalley W C, Li Li, Lyyra A M and Amiot C 1996 *J. Chem. Phys.* **105** 7976
[31] Smirnov B M and Chibisov M I 1965 *Sov. Phys.—JETP* **21** 624
[32] Goral K, Koehler T, Gardiner S A, Tiesinga E and Julienne P S 2004 *J. Phys. B: At. Mol. Opt. Phys.* **37** 3457
[33] Marinescu M, Sadeghpour H R and Dalgarno A 1994 *Phys. Rev.* A **49** 982
[34] Esry B D, Greene C H and Burke J P Jr 1999 *Phys. Rev. Lett.* **83** 1751
[35] Petrov D S, Salomon C and Shlyapnikov G V 2005 *Phys. Rev.* A **71** 012708
[36] Thalhammer G, Winkler K, Lang F, Schmid S, Grimm R and Hecker Denschlag J 2006 *Phys. Rev. Lett.* **96** 050402